

Defect-induced magnetism in TiO_2 : An example of quasi 2D magnetic order with perpendicular anisotropy

Markus Stiller[†] and Pablo D. Esquinazi^{*}

*Division of Quantum Magnetism and Superconductivity,
Felix Bloch Institute for Solid State Physics, Faculty of Physics and Earth Sciences,
University of Leipzig, Linnéstrasse 5, D-04103 Leipzig, Germany*

Magnetic order at room temperature induced by atomic lattice defects, like vacancies, interstitials or pairs of them, has been observed in a large number of different nonmagnetic hosts, such as pure graphite, oxides and silicon-based materials. High Curie temperatures and time independent magnetic response at room temperature indicate the extraordinary robustness of this new phenomenon in solid state magnetism. In this work, we review experimental and theoretical results in pure TiO_2 (anatase), which magnetic order can be triggered by low-energy ion irradiation. In particular, we discuss the systematic observation of an ultrathin magnetic layer with perpendicular magnetic anisotropy at the surface of this oxide.

*: esquin@physik.uni-leipzig.de

†: Current address: zollsoft GmbH, Jena, Germany. Email: markus@mstiller.org

I. INTRODUCTION TO DEFECT-INDUCED MAGNETISM

Till not so far away in time, solid state physicists and materials scientists were convinced that to get magnetic order in a solid one needs a certain amount of magnetic ions, like Fe, Ni, etc., in the atomic lattice. Their amount as well as their environment have a direct influence in the magnetic ordering temperature, i.e., the Curie temperature. This concept was and still is successfully applied in basic and applied research to get magnetic order in solids, since Heisenberg introduced the idea of exchange interaction between the electron orbits of neighbor magnetic ions [1]. Actually, the changes in the electron orbits produced by a defect, such as a vacancy in its environment, can be substantially large. Therefore, these changes can lead to a non-negligible probability to have a significant local magnetic moment, see e.g. [2–9]. To get magnetic order in a solid through atomic lattice defects or through doping of non magnetic ions we need to reach a minimum defect density of the order of (or larger than) ~ 5 at.%. The reason is that at this or higher density, the exchange coupling mechanism between the localized magnetic moments at the defects gets robust enough to trigger the alignment between them.

Defect engineering is also of importance in two-dimensional samples, as in transition-metal dichalcogenides materials, see, e.g., the review in [10]. Moreover, magnetic order through Se-vacancies has been recently demonstrated in monolayer VSe_2 [11]. Ion irradiation can be used in this case to systematically produce a certain kind of vacancy by appropriately choosing the ion and its energy.

II. EMERGING FERROMAGNETIC PHASE THROUGH ION IRRADIATION

Ion irradiation is a sophisticated method to produce atomic lattice defects systematically at certain positions and a given density. The main difference between the irradiation of a solid with different kinds of ions (including protons and electrons) is given by their penetration depth, density and type of atomic lattice defects produced upon selected energies. Several works on the subject were published in the past, see e.g. Refs. [12–18] with Curie temperatures up to 880 K [16, 19].

The possibility to trigger local magnetic moments up to magnetic order by particle irradiation on a given solid, whatever its structure, is significant. Starting with proton irradiation of graphite [20–23] and ZnO [4] to Ar^+ irradiation of TiO_2 [24, 25], the amount of published works using irradiation to trigger magnetic order increases steadily.

In this section we would like to discuss general results following the theoretical works described in Refs. [25, 26]. In particular we discuss here the emergence of the two-dimensional magnetic order at the surface of TiO_2 in its anatase structure, obtained assuming Ar^+ irradiation at low energies $\lesssim 200$ eV. In general, after ion irradiation with the corresponding fluence and energy to trigger magnetic order, the defect density remains below a threshold where amorphicity grows all over the sample. The magnetic order is in general observed directly after ion irradiation without any further (thermal) treatment.

Which are the main magnetic defects one produces in TiO_2 by Ar^+ irradiation? From the molecular dynamics simulations of collision cascades in anatase TiO_2 given in [25–27], the primary magnetic defects are the so-called di-Frenkel pairs (dFP), consisting of two Ti atoms displaced into interstitial sites leaving behind two vacancies. Also oxygen vacancies O_v are created. With the help of density functional theory (DFT) calculations, the

magnetic moment of a dFP has been calculated to be $2 \mu_B$ [26] and $1 \mu_B$ [28] for the O_v . The defect formation probabilities for these defects, calculated in [27], are large ($\sim 40\%$ and $\sim 50\%$, respectively). A diagram of

these probabilities also for other defects in anatase TiO_2 can be seen in Fig. 8 in [25]). With the knowledge of these probabilities and using the program SRIM [29] a magnetic phase diagram can be proposed.

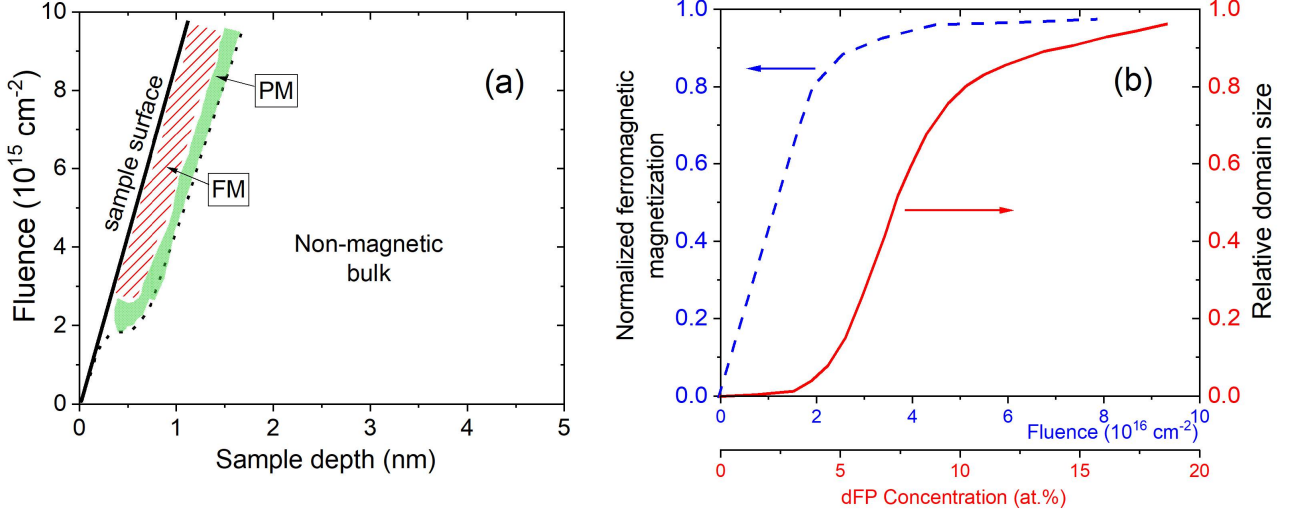


Fig. 1. (a) Semiquantitative magnetic phase diagram (fluence vs. sample depth) for a TiO_2 anatase sample irradiated with Ar^+ ions of 200 eV energy following the results of [25]. The straight line denotes the position of the sample surface, which shifts due to the sputtering. The red region is the ferromagnetic (FM) region and the green a paramagnetic (PM) one. The dotted line represents roughly the transition region between a PM and a non-magnetic one, where the mean number of defects created by the irradiation is negligible. The dotted line can be considered as the penetration depth of the irradiated ions. (b) Blue dashed line: Normalized ferromagnetic magnetization vs. Ar^+ fluence or the estimated dFP density in TiO_2 anatase phase. Red line: Relative FM domain size vs. fluence or dFP concentration. The curves represent semiquantitatively the main theoretical results from [25] for the case of irradiation of Ar^+ -ions with 200 eV energy in TiO_2 anatase phase.

Figure 1(a) shows diagrammatically the magnetic phases we expect as a function of the used fluence and sample depth. The magnetic phase diagram resumes the results obtained by [25] for TiO_2 anatase using Ar^+ ions. The absolute values included in the magnetic phase diagram of Fig. 1 roughly correspond to the case we discuss here (Ar^+ ions at an energy of ~ 200 eV). The straight line in Fig. 1(a) represents the evolution of the surface position of the TiO_2 sample (which represents a decrease of the total sample thickness), when the ion fluence increases. The main reason for this behavior is surface sputtering, non negligible at low ion energies. Roughly speaking, using SRIM [29] the estimated sputtering is $\sim 1 \text{ nm}/(10^{16} \text{ ion}/\text{cm}^2)$ [25]. Due to the sputtering the amorphous surface layer produced by the irradiation is continuously removed. Following [25], from a fluence value $\sim 4 \times 10^{15} \text{ cm}^{-2}$ the defect creation and sputtering processes reach equilibrium where the volume (and defect density) of the emerging FM phase (red region in Fig. 1(a)) remains constant over the whole fluence range above this value. In this regime the thickness of the FM phase reaches a value of $d_{FM} \simeq 0.46 \text{ nm}$, which is about $1/2$ of the anatase lattice constant $c = 0.951 \text{ nm}$ along the (001) crystal direction. It means that with an irradiation energy of ~ 200 eV we expect to have an emerging

FM phase at the first \sim two layers of the TiO_2 lattice at its surface.

Deeper in the sample, beyond the $\sim 0.5 \text{ nm}$ thick FM layer, the density of magnetic defects decreases below the required minimum ($\sim 5\%$) to get FM. Instead, a paramagnetic (PM) phase appears (green region in Figure 1(a)). The dotted line in the diagram represents the transition region between PM and the non-magnetic bulk, which can be interpreted as the mean penetration depth of the Ar^+ ions at 200 eV.

Increasing the defect density we expect a transition from isolated local magnetic moments to a long-ranged ordered phase. How much of the dFP defects are created in the TiO_2 anatase atomic lattice within the FM phase? This depends on the length-scale of the exchange coupling, which determines whether two localized magnetic moments (the dFP in the case of TiO_2) are close enough to each other to interact ferromagnetically. Ref. [25] answered this question within the framework of percolation theory and the main results are shown diagrammatically in Fig. 1(b). It semiquantitatively shows the theoretical results [25] on the evolution of the FM magnetization and the relative domain size as a function of dFP concentration or fluence for the irradiation of Ar^+ -ions at 200 eV. Single pairs of defects interacting ferromagnetically build

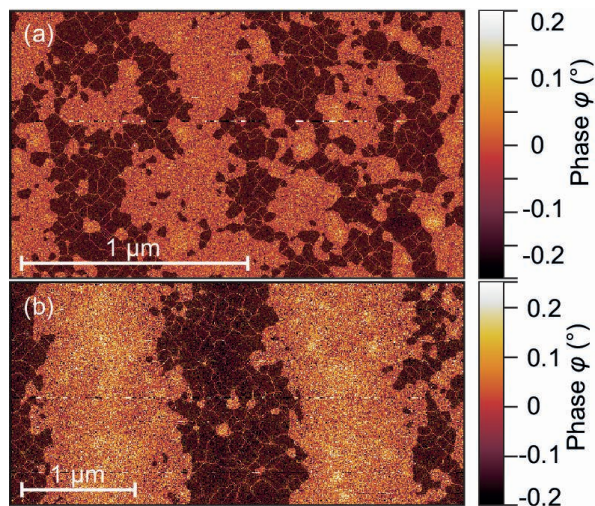


Fig. 2. Magnetic force microscopy measurements at two different positions (a) and (b) of a fully irradiated and otherwise untreated anatase thin film. The TiO_2 thin film was irradiated with Ar^+ -ions with a fluence $\sim 10^{16} \text{ cm}^{-2}$ and 200 eV energy. The magnetic domains have been segmented with a barrier of 40% and a Gaussian smoothing factor of 8px.

the smallest ferromagnetic domain. Increasing the defect density the size of the domains grows as shown by the red line in Fig. 1(b). For a density of Frenkel pairs $\text{dFP} \gtrsim 10 \text{ at.}\%$, the domain size tends to saturate at the sample size (relative domain size 1). At this defect concentration the FM magnetization (blue dashed line in Fig. 1(b)) tends to reach its saturation.

The magnetic percolation transition as a function of the fluence of Ar^+ -ions (or defect density), was experimentally verified by measuring the remanent magnetic moment at zero field of TiO_2 thin films as a function of the fluence. It follows the expected critical behavior for a percolation transition of a magnetic bilayer system (see Fig. 13 in [25]). In the next section we review the experimental evidence for the appearance of this 2D magnetic system with the interesting property of having the magnetization easy-axis normal to the main sample surface.

III. EVIDENCE FOR A TWO-DIMENSIONAL FERROMAGNETIC PHASE WITH OUT-OF-PLANE EASY AXIS

A. Reasons for the magnetic anisotropy

As indicated above, following theoretical and experimental results, at a low ion energy of 200 eV the magnetically ordered phase appears at the first two layers of the TiO_2 anatase surface. If we irradiate TiO_2 with Ar^+ -ions of higher energy (e.g., 500 eV), the magnetic anisotropy changes and the magnetization easy-axis points parallel to the sample surface [25, 26]. This

evidence clearly indicates that the negative magnetic anisotropy energy (MAE) found at low irradiation energies is directly related to the two-dimensionality of the ferromagnetic phase produced at the surface of the TiO_2 sample. The localized magnetic moments of the dFP defect at the (001) anatase surface of the measured samples are at the two interstitial Ti places. One of them $\text{Ti}_{i,2}$ is located at the first surface layer, whereas the other interstitial $\text{Ti}_{i,1}$ on the second layer. According to DFT electronic structure calculations using the full potential linearized augmented plane wave (FLAPW) method, the magnetic defect $\text{Ti}_{i,1}$ shows a similar spin structure as in the bulk. Whereas the $\text{Ti}_{i,2}$ defect shows a completely different spin polarization with a negative MAE due to the reduced coordination of the surface [25]. Increasing the magnetically ordered volume inside the sample by increasing the irradiation energy, the smaller is the relative contribution of this magnetic surface to the total magnetization and the magnetic anisotropy turns to positive.

The first clear hints for the unusual magnetic anisotropy of the TiO_2 thin films after irradiation were obtained by SQUID angle dependent magnetization measurements [24]. This interesting finding was supported a few years later through similar SQUID measurements of new TiO_2 thin films irradiated at different energies [25, 26]. We would like to emphasize the main results obtained from magnetic hysteresis loops obtained applying external magnetic fields parallel and perpendicular to the film surface of irradiated TiO_2 samples using a SQUID magnetometer. The total magnetic anisotropy energy was obtained from the difference between the areas of the two first field (virgin) dependent curves, for more details see Ref. [25] and its supplementary information [30]. The magnetization results show that the MAE for the 200 eV Ar^+ irradiated sample is negative with a value of $\text{MAE} \sim -0.03 \text{ mJ/cm}^2$ nearly independent of the irradiated fluence up to $\sim 3 \times 10^{16} \text{ cm}^{-2}$ [25], in agreement with the predicted behavior given by the red area in Fig. 1(a). In the next section we discuss the visualization of magnetic domains via MFM, supporting the anomalous MAE of irradiated TiO_2 . It is worth to note that perpendicular magnetic anisotropy has been reported in monolayers of Cr_3Te_4 , triggered in this case not by atomic lattice defects in the material itself but by an interfacial effect between the monolayer and graphite [31].

B. Magnetic Force Microscopy

Thin films of anatase, prepared by pulsed laser deposition on LaAlO_3 substrate, have been irradiated with low energy ions, and measured using magnetic force microscopy (MFM) [26]. Previously conducted SQUID measurements show a low remanence, thus we expect randomly distributed magnetic domains at the anatase surface. Figures 2(a) and (b) show MFM measurements at two different positions, and the magnetic domains as

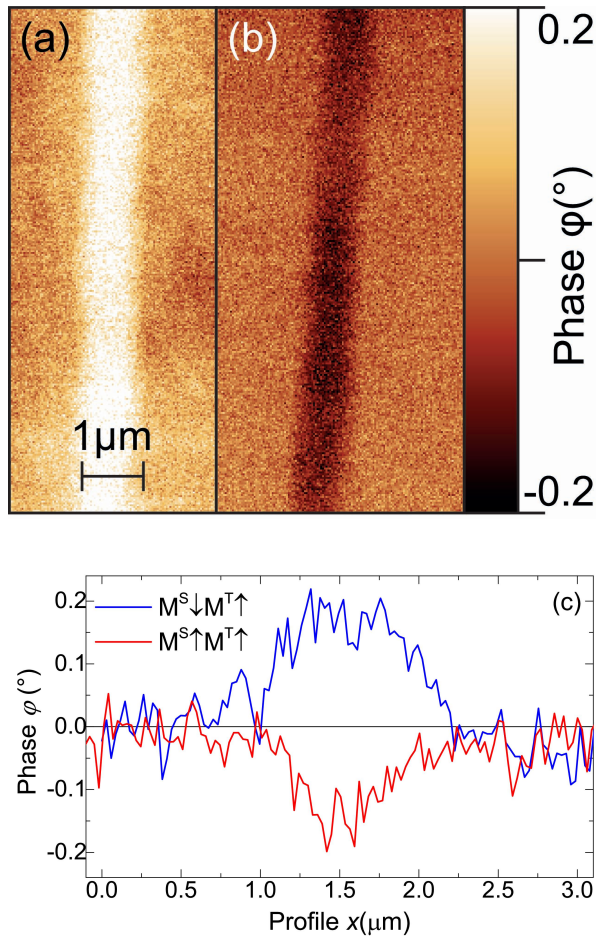


Fig. 3. Magnetic force microscopy measurements with the sample (M^S) and tip (M^T) magnetization antiparallel (a) and parallel (b) with respect to each other; (c) shows the corresponding line scans.

well as their out-of-plane character can clearly be recognized. An in-plane domain structure would only be visible at the domain walls as the out-of-plane field vanishes within the domains.

In order to examine the possibility for controlled magnetic manipulation at the surface of the anatase thin film,

the samples were patterned using electron beam lithography. Therefore, a film was covered with a resist, and electron beam lithography was used to prepare a mask. The resulting irradiated lines or stripes have a width of ≈ 750 nm. After irradiation with low energy argon ions, the whole mask was completely removed and the sample was magnetized using a permanent magnet with a magnetic field aligned perpendicular to the sample surface and two magnetization directions; parallel and antiparallel to the tip magnetization. No external field was applied during the measurement[26]. The results are shown in Figures 3(a) and (b), and present a clear MFM signal corresponding to the two out-of-plane magnetic field directions; the area of the thin film which was not irradiated does not show any MFM response. Phase line scans normal to the main length of the FM stripes shown in Figs. 3(a) and (b), are shown in Fig. 3(c).

IV. CONCLUSION

In conclusion, it has been shown that ferromagnetism at room temperature with perpendicular magnetic anisotropy can be induced in anatase after irradiating the sample with low-energy ions. The used method is remarkably simple and cheap compared to other experimental methods to produce perpendicular magnetic anisotropy, such as magnetic heterostructures [32]. The irradiation strategy is similar to the doping approach used in the semiconductor industry. However, the advantage of our method relays in its efficiency and the possibility to easily combine with other techniques, as electron beam lithography, allowing the production of arbitrary magnetic patterns with 2D perpendicular magnetic anisotropy.

ACKNOWLEDGEMENTS

The authors acknowledge support from the German Research Foundation (DFG) and Universität Leipzig within the program of Open Access Publishing

-
- [1] Heisenberg W. Zur Theorie des Ferromagnetismus. *Z. Phys.* **49** (1928) 619–636.
 - [2] Khalid M, Ziese M, Setzer A, Esquinazi P, Lorenz M, Hochmuth H, et al. Defect-induced magnetic order in pure ZnO films. *Phys. Rev. B* **80** (2009) 035331. doi: <https://doi.org/10.1103/PhysRevB.80.035331>.
 - [3] Fischer G, Sanchez N, Adeagbo W, Lüders M, Szotek Z, Temmerman WM, et al. Room-temperature p-induced surface ferromagnetism: First-principles study. *Phys. Rev. B* **84** (2011) 205306.
 - [4] Lorite I, Straube B, Ohldag H, Kumar P, Villafuerte M, Esquinazi P, et al. Advances in methods to obtain and characterise room temperature magnetic ZnO. *Applied Physics Letters* **106** (2015) 082406.
 - [5] Esquinazi PD, Hergert W, Stiller M, Botsch L, Ohldag H, Spemann D, et al. Defect-induced magnetism in non-magnetic oxides: Basic principles, experimental evidence, and possible devices with ZnO and TiO₂. *Phys. Status Solidi B* (2020). doi:10.1002/pssb.201900623.
 - [6] Volnianska O, Boguslawski P. Magnetism of solids resulting from spin polarization of *p* orbitals. *J. Phys.:*

- Condens. Matter* **22** (2010) 073202. doi:10.1088/0953-8984/22/7/073202.
- [7] Ogale SB. Dilute doping, defects, and ferromagnetism in metal oxide systems. *Adv. Mater.* **22** (2010) 3125–3155. doi:https://doi.org/10.1002/adma.200903891.
 - [8] Stoneham M. The strange magnetism of oxides and carbons. *J. Phys.: Condens. Matter* **22** (2010) 074211. doi:10.1088/0953-8984/22/7/074211.
 - [9] Esquinazi P, Hergert W, Spemann D, Setzer A, Ernst A. Defect-induced magnetism in solids. *Magnetics, IEEE Transactions on* **49** (2013) 4668–4674. doi:10.1109/TMAG.2013.2255867.
 - [10] Liang Q, Zhang Q, Zhao X, Liu M, Wee ATS. Defect engineering of two-dimensional transition-metal dichalcogenides: Applications, challenges, and opportunities. *ACS Nano* **15** (2021) 2165–2181. doi:10.1021/acsnano.0c09666.
 - [11] Chua R, Yang J, He X, Yu X, Yu W, Bussolotti F, et al. Can reconstructed se-deficient line defects in monolayer vse2 induce magnetism? *Advanced Materials* **32** (2020) 2000693. doi:https://doi.org/10.1002/adma.202000693.
 - [12] Hong NH, Sakai J, Poirot N, Brizé V. Room-temperature ferromagnetism observed in undoped semiconducting and insulating oxide thin films. *Physical Review B* **73** (2006) 132404–4. doi:10.1103/PhysRevB.73.132404.
 - [13] Zhou S, Čížmár E, Potzger K, Krause M, Talut G, Helm M, et al. Origin of magnetic moments in defective TiO₂ single crystals. *Physical Review B* **79** (2009) 113201–4. doi:10.1103/PhysRevB.79.113201.
 - [14] Cruz MM, Silva RCd, Franco N, Godinho M. Ferromagnetism induced in rutile single crystals by argon and nitrogen implantation. *Journal of Physics: Condensed Matter* **21** (2009) 206002–8. doi:10.1088/0953-8984/21/20/206002.
 - [15] Thakur H, Thakur P, Kumar R, Brookes NB, Sharma KK, Singh AP, et al. Irradiation induced ferromagnetism at room temperature in TiO₂ thin films: X-ray magnetic circular dichroism characterizations. *Applied Physics Letters* **98** (2011) 192512–3. doi:10.1063/1.3592250.
 - [16] Yoon SD, Chen Y, Yang A, Goodrich TL, Zuo X, Ziemer K, et al. Magnetic semiconducting anatase TiO₂- δ grown on (100) LaAlO₃ having magnetic order up to 880K. *Journal of Magnetism and Magnetic Materials* **309** (2007) 171–175. doi:10.1016/j.jmmm.2006.05.014.
 - [17] Li DX, Qin XB, Zheng LR, Li YX, Cao XZ, Li ZX, et al. Defect types and room-temperature ferromagnetism in undoped rutile TiO₂ single crystals. *Chinese Physics B* **22** (2013) 037504–4. doi:10.1088/1674-1056/22/3/037504.
 - [18] Vázquez-Robaina O, Cabrera AF, Cruz AF, Torres CER. Observation of room-temperature ferromagnetism induced by high-pressure hydrogenation of anatase TiO₂. *J. Phys. Chem. C* **125** (2021) 14366–14377. doi:10.1021/acs.jpcc.1c00124.
 - [19] Yoon SD, Chen Y, Yang A, Goodrich TL, Zuo X, Arena DA, et al. Oxygen-defect-induced magnetism to 880 K in semiconducting anatase TiO₂- δ films. *Journal of Physics: Condensed Matter* **18** (2006) L355–L361. doi:10.1088/0953-8984/18/27/L01.
 - [20] Esquinazi P, Spemann D, Höhne R, Setzer A, Han KH, Butz T. Induced magnetic ordering by proton irradiation in graphite. *Phys. Rev. Lett.* **91** (2003) 227201. doi:https://doi.org/10.1103/PhysRevLett.91.227201.
 - [21] Ohldag H, Tylliszczak T, Höhne R, Spemann D, Esquinazi P, Ungureanu M, et al. π -electron ferromagnetism in metal-free carbon probed by soft x-ray dichroism. *Phys. Rev. Lett.* **98** (2007) 187204. doi:https://doi.org/10.1103/PhysRevLett.98.187204.
 - [22] Ohldag H, Esquinazi P, Arenholz E, Spemann D, Rothmel M, Setzer A, et al. The role of hydrogen in room-temperature ferromagnetism at graphite surfaces. *New Journal of Physics* **12** (2010) 123012. doi:http://stacks.iop.org/1367-2630/12/i=12/a=123012.
 - [23] Spemann D, Esquinazi P. *Evidence for magnetic order in graphite from magnetization and transport measurements* (P. Esquinazi (ed.), Springer International Publishing AG Switzerland). Springer Series in Materials Science 244 (2016), 45–76. doi:https://doi.org/10.1007/978-3-319-39355-1_3.
 - [24] Stiller M, Barzola-Quiquia J, Esquinazi P, Spemann D, Meijer J, Lorenz M, et al. Strong out-of-plane magnetic anisotropy in ion irradiated anatase TiO₂ thin films. *AIP Advances* **6** (2016) 125009. doi:10.1063/1.4971794.
 - [25] Botsch L, Esquinazi PD, Bundesmann C, Spemann D. Toward a systematic discovery of artificial functional magnetic materials. *Phys. Rev. B* (2021). doi:10.1103/PhysRevB.104.014428.
 - [26] Stiller M, N'Diaye AT, Ohldag H, Barzola-Quiquia J, Esquinazi PD, Amelal T, et al. Titanium 3d ferromagnetism with perpendicular anisotropy in defective anatase. *Physical Review B* **101** (2020) 014412. doi:10.1103/PhysRevB.101.014412.
 - [27] Robinson M, Marks N, Lumpkin G. Structural dependence of threshold displacement energies in rutile, anatase and brookite tio₂. *Materials Chemistry and Physics* **147** (2014) 311–318. doi:https://doi.org/10.1016/j.matchemphys.2014.05.006.
 - [28] Li QK, Wang B, Woo CH, Wang H, Zhu ZY, Wang R. Origin of unexpected magnetism in Cu-doped TiO₂. *Europhysics Letters (EPL)* **81** (2007) 17004. doi:10.1209/0295-5075/81/17004.
 - [29] Ziegler JF, Biersack JP, Ziegler MD. *SRIM - The Stopping and Range of Ions in Matter* (SRIM Co.) (2008). ISBN 0-9654207-1-X. See also the simulation software IIS available at <http://www.ele.uva.es/~jesman/iis.html>, which has some advantages in comparison with the usual SRIM simulation.
 - [30] Botsch L, Esquinazi PD, Bundesmann C, Spemann D. Supplemental material (2021). See Supplemental Material at <http://link.aps.org/supplemental/10.1103/PhysRevB.104.014428> for full magnetic hysteresis curves and details on obtaining the magnetic anisotropy energy.
 - [31] Chua R, Zhou J, Yu X, Yu W, Gou J, Zhu R, et al. Room temperature ferromagnetism of monolayer chromium telluride with perpendicular magnetic anisotropy. *Advanced Materials* **33** (2021) 2103360. doi:https://doi.org/10.1002/adma.202103360.
 - [32] Li W, Zeng Y, Zhao Z, Zhang B, Xu J, Huang X, et al. 2D magnetic heterostructures and their interface modulated magnetism. *ACS Appl. Mater. Interfaces* **13** (2021) 50591–50601. doi:10.1021/acsaami.1c11132.

FUNDING

Part of this study was supported by the DFG, Project No. 31047526, SFB 762 “Functionality of oxide interfaces,” project B1.

ACKNOWLEDGMENTS

The authors thank L. Botsch and W. Hergert for the discussions, cooperation and support.